

MSSM with Non-holomorphic Soft Interactions

Utpal Chattopadhyay,
School of Physical Sciences,
Indian Association for the Cultivation of Science,
Kolkata, India

[Ref.: UC, **Abhishek Dey**, JHEP 1610 (2016) 027, arXiv:1604.06367],
[UC, **Asesh Krishna Datta**, **Samadrita Mukherjee**, **Abhaya Kumar Swain**, JHEP
1810 (2018) 202, arXiv: 1809.05438]

IMHEP 2019, IOP, Bhubaneswar, January 17, 2019



MSSM

- MSSM Superpotential and soft SUSY breaking terms::

$$\mathcal{W} = \mu H_D \cdot H_U - Y_{ij}^e H_D \cdot L_i \bar{E}_j - Y_{ij}^d H_D \cdot Q_i \bar{D}_j - Y_{ij}^u Q_i \cdot H_U \bar{U}_j$$

$$A \cdot B = \epsilon_{\alpha\beta} A^\alpha B^\beta$$

$$\begin{aligned} -\mathcal{L}_{\text{soft}} &= [\tilde{q}_{iL} \cdot h_u (A_u)_{ij} \tilde{u}_{jR}^* + h_d \cdot \tilde{q}_{iL} (A_d)_{ij} \tilde{d}_{jR}^* + h_d \cdot \tilde{l}_{iL} (A_e)_{ij} \tilde{e}_{jR}^* + h.c.] \\ &+ (B\mu h_d \cdot h_u + h.c.) + m_d^2 |h_d|^2 + m_u^2 |h_u|^2 \\ &+ \tilde{q}_{iL}^* (M_{\tilde{q}}^2)_{ij} + \tilde{u}_{iR}^* (M_{\tilde{u}}^2)_{ij} \tilde{u}_{jR} + \tilde{d}_{iR}^* (M_{\tilde{d}}^2)_{ij} \tilde{d}_{jR} + \tilde{l}_{iL}^* (M_{\tilde{l}}^2)_{ij} \tilde{l}_{jL} \\ &+ \text{gaugino mass terms} \end{aligned}$$

- Possible origin of soft terms: SUSY breaking parametrized by vev of F -term of a chiral superfield X , so that $\langle X \rangle = \theta\theta \langle F \rangle \equiv \theta\theta F$. X couples to Φ and a gauge strength superfield W_α .

Type	Term	Naive Suppression	Origin
soft	$\phi\phi^*$	$\frac{ F ^2}{M^2} \sim m_W^2$	$\frac{1}{M^2} [XX^*\Phi\Phi^*]_D$
	ϕ^2	$\frac{\mu F}{M} \sim \mu m_W$	$\frac{\mu}{M} [X\Phi^2]_F$
	ϕ^3	$\frac{F}{M} \sim m_W$	$\frac{1}{M} [X\Phi^3]_F$
	$\lambda\lambda$	$\frac{F}{M} \sim m_W$	$\frac{1}{M} [XW^\alpha W_\alpha]_F$

- Are there any more possible soft terms ?

Nonholomorphic soft SUSY breaking terms

- ▶ S. Martin, Phys. Rev D., 2000; Possible non-holomorphic soft SUSY breaking terms:

Type	Term	Naive Suppression	Origin
"maybe soft"	$\phi^2 \phi^*$	$\frac{ F ^2}{M^3} \sim \frac{m_W^2}{M}$	$\frac{1}{M^3} [XX^* \Phi^2 \Phi^*]_D$
	$\psi\psi$	$\frac{ F ^2}{M^3} \sim \frac{m_W^2}{M}$	$\frac{1}{M^3} [XX^* D^\alpha \Phi D_\alpha \Phi]_D$
	$\psi\lambda$	$\frac{ F ^2}{M^3} \sim \frac{m_W^2}{M}$	$\frac{1}{M^3} [XX^* D^\alpha \Phi W_\alpha]_D$

- ▶ "maybe soft": *In the absence of any gauge singlet scalar* the above non-holomorphic terms are of soft SUSY breaking in nature. But, these have mass scale suppression by M .
- ▶ A gauge singlet scalar field would have **tadpole contributions** causing **hard SUSY breaking**.
- ▶ NHSSM: MSSM + NH terms like $\phi^2 \phi^*$ and $\psi\psi$:

$$-\mathcal{L}'_{soft} = h_d^c \cdot \tilde{q}_{iL} (A'_u)_{ij} \tilde{u}_{jR}^* + \tilde{q}_{iL} \cdot h_u^c (A'_d)_{ij} \tilde{d}_{jR}^* + \tilde{l}_{iL} \cdot h_e^c (A'_e)_{ij} \tilde{e}_{jR}^* + \mu' \tilde{h}_u \cdot \tilde{h}_d + h.c.$$

Higgs fields are replaced with their conjugates: h_d going with up-type of squarks etc.

- ▶ V_{Higgs} is unaffected. But, the potential involving charged and colored scalar fields needs a separate study for CCB.

Nonholomorphic terms: A partial list of related analyses and our present work

- ▶ **Hall and Randall**, PRL 1990, **Jack and Jones**, PRD 2000: Quasi IF fixed points and RG invariant trajectories; **Jack and Jones** PLB 2004: General analyses with NH terms involving RG evolutions.
- ▶ Works performed under Constrained MSSM (CMSSM)/minimal supergravity(mSUGRA) setup for studying the Higgs mass and observables like $\text{Br}(B \rightarrow X_s + \gamma)$ etc.: **Hetherington** JHEP 2001, **Solmaz et. al.** PRD 2005, PLB 2008, PRD 2015. The analyses involve mixed type of inputs given at the unification and electroweak scales.
- ▶ **Ross, Schmidt-Hoberg, Staub** PLB 2016, JHEP 2017. Focused on fine-tuning and higgsino DM, stressed the importance of the bilinear higgsino term identifying various scenarios.
- ▶ **UC, A. Dey** JHEP 2016: No specific mechanism for SUSY breaking: all the parameters are given at the low scale. Impact on muon $g - 2$ apart from EW fine-tuning, Higgs mass etc.
UC, D. Das, S. Mukherjee, JHEP 2018: On GMSB type of realization of NHSSM.
J. Beuria and A. Dey, JHEP 2017, CCB effects in NHSSM
UC, A. Datta, S. Mukherjee, A. K. Swain: JHEP 2018, Sbottom phenomenology.

Bilinear Higgsino soft term

- ▶ The following reparametrization of μ , μ' and Higgs scalar mass parameters may evade the need of a bilinear higgsino soft term.
 $\mu \rightarrow \mu + \delta$, $\mu' \rightarrow \mu' + \delta$, and $m_{H_{U,D}}^2 \rightarrow m_{H_{U,D}}^2 - 2\mu\delta - \delta^2$
- ▶ A reparametrization would however involve *ad-hoc* correlations between unrelated parameters [Jack and Jones 1999, Hetherington 2001 etc.].
- ▶ Such correlations are arbitrary, at least in view of fine-tuning. In particular, there may be a scenario where definite SUSY breaking mechanisms generate bilinear higgsino soft terms whereas it may keep the scalar sector unaffected. [Ross *et. al.* 2016, 2017, Antoniadis *et. al.* 2008, Perez *et. al.* 2008 etc].
- ▶ The μ' term that is traditionally retained, isolates a fine-tuning measure (typically $\sim \text{factor} \times \mu^2/M_Z^2$) from the higgsino mass ($\mu + \mu'$): \Rightarrow Possibility of a large higgsino mass (like a TeV satisfying DM relic limits) while having a small fine-tuning.

In a general standpoint we acknowledge the importance of trilinear and bilinear NH soft terms, irrespective of a suppression predicted by a *given* model. Unlike other analyses, we will use a pMSSM type of work on Non-holomorphic supersymmetric SM (NHSSM).

NHSSM: scalars and electroweakinos

► Squarks : $M_{\tilde{u}}^2 = \begin{bmatrix} m_{\tilde{Q}}^2 + (\frac{1}{2} - \frac{2}{3} \sin^2 \theta_W) M_Z^2 \cos 2\beta + m_u^2 & -m_u(A_u - (\mu + A'_u) \cot \beta) \\ -m_u(A_u - (\mu + A'_u) \cot \beta) & m_{\tilde{u}}^2 + \frac{2}{3} \sin^2 \theta_W M_Z^2 \cos 2\beta + m_u^2 \end{bmatrix},$

Sleptons (off-diagonal): $-m_\mu[A_\mu - (\mu + A'_\mu) \tan \beta] \Rightarrow A'_\mu \tan \beta$ **potentially enhances** $(g - 2)_\mu^{\text{SUSY}}$, particularly affecting the $\tilde{\chi}_1^0 - \tilde{\mu}$ loop contributions.

► Higgs mass corrections : $\Delta m_{h, \text{top}}^2 = \frac{3g_2^2 \bar{m}_t^4}{8\pi^2 M_W^2} \left[\ln \left(\frac{m_{\tilde{t}_1} m_{\tilde{t}_2}}{\bar{m}_t^2} \right) + \frac{X_t^2}{m_{\tilde{t}_1} m_{\tilde{t}_2}} \left(1 - \frac{X_t^2}{12m_{\tilde{t}_1} m_{\tilde{t}_2}} \right) \right],$

Here, $X_t = A_t - (\mu + A'_t) \cot \beta \Rightarrow$ influence on m_h .

► Charginos : $M_{\tilde{\chi}^\pm} = \begin{pmatrix} M_2 & \sqrt{2}M_W \sin \beta \\ \sqrt{2}M_W \cos \beta & -(\mu + \mu') \end{pmatrix},$

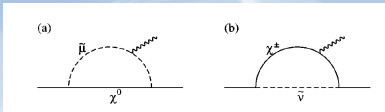
$m_{\tilde{\chi}_1^\pm} \gtrsim 100 \text{ GeV} \Rightarrow |\mu + \mu'| \gtrsim 100 \text{ GeV}$. Muon $g - 2$ may be enhanced via a light higgsino.

► Neutralinos : $M_{\tilde{\chi}^0} = \begin{pmatrix} M_1 & 0 & -M_Z \cos \beta \sin \theta_W & M_Z \sin \beta \sin \theta_W \\ 0 & M_2 & M_Z \cos \beta \cos \theta_W & -M_Z \sin \beta \cos \theta_W \\ -M_Z \cos \beta \sin \theta_W & M_Z \cos \beta \cos \theta_W & 0 & -(\mu + \mu') \\ M_Z \sin \beta \sin \theta_W & -M_Z \sin \beta \cos \theta_W & -(\mu + \mu') & 0 \end{pmatrix}$

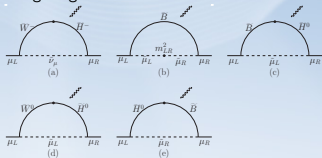
► If $|(\mu + \mu')| \ll M_1, M_2 \Rightarrow \tilde{\chi}_1^0$ is higgsino-like. It is possible to have an acceptable higgsino-like LSP with small μ (\sim i.e. small electroweak fine-tuning.)

Muon anomalous magnetic moment: $(g - 2)_\mu$ in MSSM

- ▶ Large discrepancy from the SM (more than 3σ): $a_\mu^{exp} - a_\mu^{SM} = (29.3 \pm 8) \times 10^{-10}$
- ▶ MSSM contributions to muon $(g-2)$: Diagrams involving charginos and neutralinos



Gauge Eigenstate basis:



- ▶ Slepton L-R mixing in MSSM:
 $m_\mu(A_\mu - \mu \tan \beta)$

- ▶ The mixing influences the last item of Δa_μ shown in blue. Typically, A_μ is quite smaller than $\mu \tan \beta$, especially for large $\tan \beta$.

- ▶ In NHSSM: $m_\mu [(A_\mu - A'_\mu \tan \beta) - \mu \tan \beta]$
 A'_μ effect is enhanced by $\tan \beta$ causing a significant change in Δa_μ .

$$\Delta a_\mu(\tilde{W}, \tilde{H}, \tilde{\nu}_\mu) \simeq 15 \times 10^{-9} \left(\frac{\tan \beta}{10} \right) \left(\frac{(100 \text{ GeV})^2}{M_{2\mu}} \right) \left(\frac{f_C}{1/2} \right),$$

$$\Delta a_\mu(\tilde{W}, \tilde{H}, \tilde{\mu}_L) \simeq -2.5 \times 10^{-9} \left(\frac{\tan \beta}{10} \right) \left(\frac{(100 \text{ GeV})^2}{M_{2\mu}} \right) \left(\frac{f_N}{1/6} \right),$$

$$\Delta a_\mu(\tilde{B}, \tilde{H}, \tilde{\mu}_L) \simeq 0.76 \times 10^{-9} \left(\frac{\tan \beta}{10} \right) \left(\frac{(100 \text{ GeV})^2}{M_{1\mu}} \right) \left(\frac{f_N}{1/6} \right),$$

$$\Delta a_\mu(\tilde{B}, \tilde{H}, \tilde{\mu}_R) \simeq -1.5 \times 10^{-9} \left(\frac{\tan \beta}{10} \right) \left(\frac{(100 \text{ GeV})^2}{M_{1\mu}} \right) \left(\frac{f_N}{1/6} \right),$$

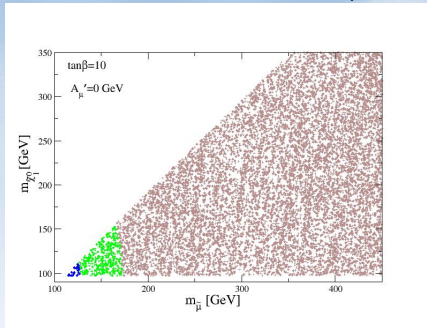
$$\Delta a_\mu(\tilde{\mu}_L, \tilde{\mu}_R, \tilde{B}) \simeq 1.5 \times 10^{-9} \left(\frac{\tan \beta}{10} \right) \left(\frac{(100 \text{ GeV})^2}{m_{\tilde{\mu}_L}^2 m_{\tilde{\mu}_R}^2 / M_{1\mu}} \right) \left(\frac{f_N}{1/6} \right).$$

[Ref. arXiv 1303.4256 by Endo, Hamaguchi, Iwamoto, Yoshinaga]

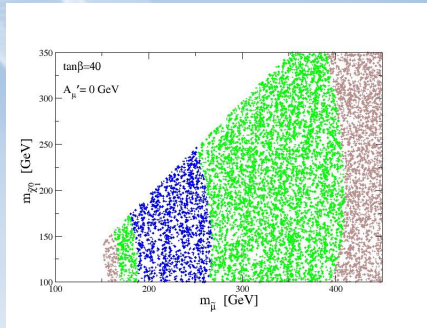
Results of muon $g-2$ in MSSM

Ref: UC, **A Dey**, *JHEP* 1610 (2016) 027, *arXiv:1604.06367*

For a parameter point enhancing muon $g-2$ upto 1σ level via smuon L-R mixing effect, the smuon mass is quite small (~ 125 GeV or 200 GeV for $\tan\beta = 10$ and 40 respectively.)



Plot in $m_{\tilde{\chi}_1^0}$ vs $m_{\tilde{\mu}_1}$ plane for $\tan\beta = 10$



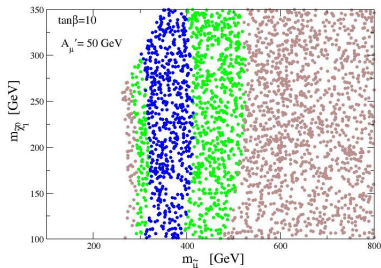
Same for $\tan\beta = 40$.

$\mu = 500$ GeV and $M_2 = 1500$ GeV. Blue, green and brown regions satisfy the muon $g-2$ constraint at 1σ , 2σ and 3σ levels respectively. All the squark and stau masses are set at 1 TeV. All trilinear parameters are zero except $A_t = -1.5$ TeV that is favorable to satisfy the Higgs mass data. **Only very light smuon can satisfy the muon $g-2$ constraint at 1σ for $\tan\beta = 10$. The upper limit of $m_{\tilde{\mu}_1}$ is about 250 GeV for $\tan\beta = 40$.**

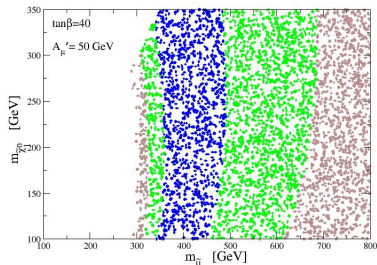
Results of muon $g-2$ in NHSSM

$$A'_{\mu} = 50 \text{ GeV.}$$

A large increase of SUSY contribution to muon $g-2$ due to enhancement effect via A'_{μ} that is multiplied by $\tan \beta$.



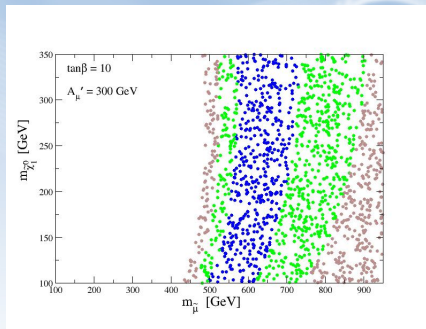
$m_{\tilde{\chi}_1^0}$ vs $m_{\tilde{\mu}_1}$ plane for $\tan \beta = 10$.
Upper limit of $m_{\tilde{\mu}_1}$: 400 GeV at 1σ .



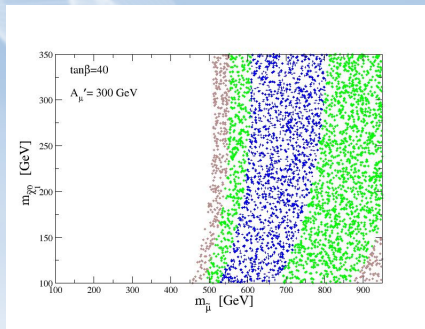
Same for $\tan \beta = 40$.
Upper limit of $m_{\tilde{\mu}_1}$: 500 GeV at 1σ

Results of muon g-2 in NHSSM

$$A'_{\mu} = 300 \text{ GeV}$$



$m_{\tilde{\chi}_1^0}$ vs $m_{\tilde{\mu}_1}$ plane for $\tan\beta = 10$.
Upper limit of $m_{\tilde{\mu}_1}$: 700 GeV at 1σ .

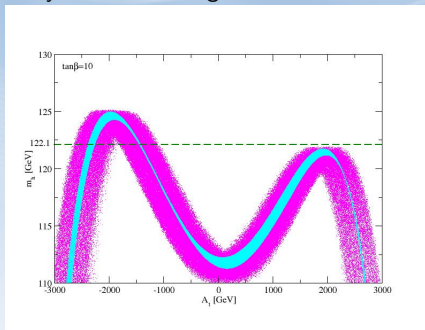


Same for $\tan\beta = 40$. Upper limit of
 $m_{\tilde{\mu}_1}$: 800 GeV at 1σ .

Impact of non-holomorphic soft parameters on m_h

A 2 to 3 GeV change in m_h can be possible via A'_t . The effect is larger for a smaller $\tan\beta$.

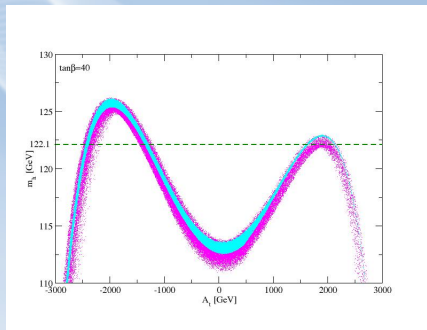
Cyan:MSSM, Magenta:NHSSM



m_h is enhanced/decreased by 2-3 GeV due to non-holomorphic terms.

• **Correct m_h possible for significantly smaller $|A_t|$.**

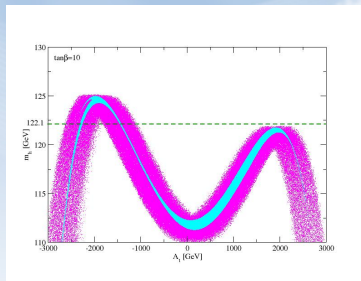
- $0 \leq \mu \leq 1$ TeV, $-2 \leq \mu' \leq 2$ TeV, $-3 \leq A'_t \leq 3$ TeV.
- A 3 GeV uncertainty in computation of m_h in SUSY is assumed.



• Since A'_t is associated with a suppression by $\tan\beta$ [off-diag term in stop sector: $X_t = A_t - (\mu + A'_t) \cot\beta$], m_h is affected only marginally.

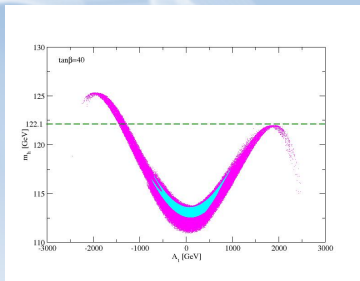
Imposing $\text{Br}(B \rightarrow X_s + \gamma)$ and $\text{Br}(B_s \rightarrow \mu^+ \mu^-)$ constraints

$$2.77 \times 10^{-4} \leq \text{Br}(B \rightarrow X_s + \gamma) \leq 4.09 \times 10^{-4}, 0.8 \times 10^{-9} \leq \text{Br}(B_s \rightarrow \mu^+ \mu^-) \leq 5 \times 10^{-9} \quad [\text{both at } 3\sigma]$$



m_h vs A_t for $\tan \beta = 10$ with the above constraints.

⇒ Essentially unaltered results for a low $\tan \beta$ like 10.



m_h vs A_t for $\tan \beta = 40$.

⇒ $\text{Br}(B \rightarrow X_s + \gamma)$ that increases with $\tan \beta$ takes away large $|A_t|$ zones of MSSM (cyan). Large $|A_t|$ with $\mu A_t < 0$ is discarded via the lower bound and vice versa. Thus m_h does not reach the desired limit beyond $|A_t| \sim 1$ TeV in MSSM.

NHSSM: The effect of A_t' is via L-R mixing:

$[A_t \rightarrow A_t - (\mu + A_t') \cot \beta]$. Thus large $|A_t|$ regions are valid via $\text{Br}(B \rightarrow X_s + \gamma)$ and m_h may stay above the desired limit.

$\text{Br}(B_s \rightarrow \mu^+ \mu^-)$ limits are not important once $\text{Br}(B \rightarrow X_s + \gamma)$ constraint is imposed.

Electroweak fine-tuning in MSSM

EWSB conditions out of minimization of V_{Higgs} :

$$\frac{m_Z^2}{2} = \frac{m_{H_d}^2 - m_{H_u}^2 \tan^2 \beta}{\tan^2 \beta - 1} - |\mu|^2, \quad \sin 2\beta = \frac{2b}{m_{H_d}^2 + m_{H_u}^2 + 2|\mu|^2} \quad (1)$$

Electroweak Fine-tuning:

$$\Delta_{p_i} = \left| \frac{\partial \ln m_Z^2(p_i)}{\partial \ln p_i} \right|, \quad \Delta_{\text{Total}} = \sqrt{\sum_i \Delta_{p_i}^2}, \text{ where } p_i \equiv \{\mu^2, b, m_{H_u}, m_{H_d}\}$$

- ▶ For $\tan \beta$ and μ both not too small the most important term is $\Delta(\mu) \simeq \frac{4\mu^2}{m_Z^2}$.
For a moderately large $\tan \beta$, a small μ means a small Δ_{Total} .
- ▶ NH soft terms do not contribute to V_{Higgs} at the tree level. Possibility of small μ with a larger higgsino LSP mass $\sim |\mu + \mu'|$ satisfying the DM data (as a single component one). This is unlike MSSM.

Probing NHSSM via sbottom decay at the LHC: Outline

Ref: UC, AseshKrishna Datta, Samadrita Mukherjee, Abhaya Kumar Swain, JHEP 1810 (2018) 202, arXiv: 1809.05438

- ▶ \tilde{b}_1 pair production and decay leading to $2b + \cancel{E}_T$ via $\tilde{b}_1 \rightarrow b + \tilde{\chi}_1^0$. Other decay modes can be $\tilde{b}_1 \rightarrow t + \tilde{\chi}_1^-$ and $\tilde{b}_1 \rightarrow \tilde{t}_1 + W^-$. Kinematic elimination used for $\tilde{b}_1 \rightarrow \tilde{t}_1 + W^-$.
- ▶ Higgsino dominated $\tilde{\chi}_1^0$ ($\mu \leq 350$ GeV) is generally considered for naturalness. $\mu' = 0$ is chosen in the main body of the analysis for simplicity.
- ▶ We keep the left and the right mass parameters $m_{\tilde{b}_L}$ and $m_{\tilde{b}_R}$ to be the same. \Rightarrow For no mixing, \tilde{b}_1 and \tilde{b}_2 are very close to L and R like respectively with effectively equal masses. With $A_b = 0$, mixing occurs via $(\mu + A'_b)$ that itself is associated with a $\tan\beta$ enhancement.
- ▶ A significant amount of radiative correction may change y_b in NHSSM. This, not only may affect the L-R mixing but may also change couplings concerned with the above electroweakinos and quarks in the \tilde{b}_i decay modes.
- ▶ Parton-level yields for $(\sigma_{\tilde{b}_1\tilde{b}_1} \times \text{BR}[\tilde{b}_1 \rightarrow b\tilde{\chi}_1^0]^2)$ in the final state $2b + \cancel{E}_T$ arising from pair-produced \tilde{b}_1 at the 13 TeV run are compared for NHSSM and MSSM for varying A'_b . Parameter space explored for large yield ratios.

- ▶ Analysis is extended to involve \tilde{b}_2 . Comparison made with MSSM with proper ratio of yields involving \tilde{b}_1 and \tilde{b}_2 pair productions and decay into $2b + \cancel{E}_T$.
- ▶ Analysis is extended to varying $m_{\tilde{b}_L}$ and $m_{\tilde{b}_R}$.
- ▶ Implications on stop searches are probed in relation to appearance of large y_b via radiative effects that may affect $\tilde{t}_1 \rightarrow b\tilde{\chi}_1^+$.

Stepwise analysis involves understanding how the relevant couplings behave while A'_b changes. Consequently, one investigates how the branching ratios $\text{Br}(\tilde{b}_1 \rightarrow b + \tilde{\chi}_1^0)$ and $\text{Br}(\tilde{b}_1 \rightarrow t + \tilde{\chi}_1^\pm)$ are affected and finally how the yields vary for changing A'_b .

MSSM and NHSSM corrections to y_b

$$\Delta m_b^{(\tilde{g})} \text{ MSSM} = \frac{2\alpha_3}{3\pi} m_{\tilde{g}} \mu y_b \frac{v_u}{\sqrt{2}} I(m_{b_1}^2, m_{b_2}^2, m_{\tilde{g}}^2),$$

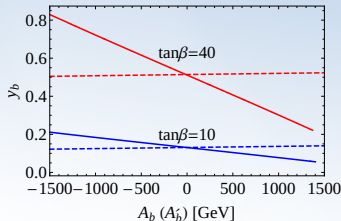
$$\Delta m_b^{\tilde{h}^+} \text{ MSSM} = \frac{y_t y_b}{16\pi^2} \mu A_t y_t \frac{v_u}{\sqrt{2}} I(m_{\tilde{t}_1}^2, m_{\tilde{t}_2}^2, \mu^2),$$

$$\Delta m_b^{(\tilde{g})} \text{ NHSSM} = \frac{2\alpha_3}{3\pi} m_{\tilde{g}} A'_b y_b \frac{v_u}{\sqrt{2}} I(m_{b_1}^2, m_{b_2}^2, m_{\tilde{g}}^2),$$

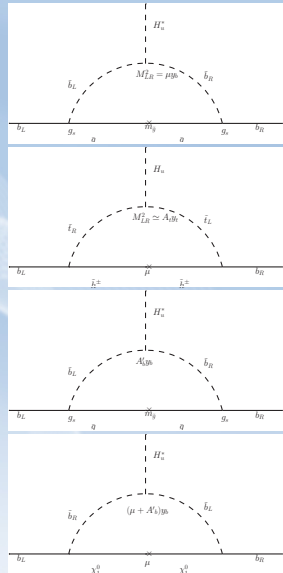
$$\Delta m_b^{\tilde{h}^0} \text{ NHSSM} = \frac{y_b^2}{16\pi^2} \mu (\mu + A'_b) y_b \frac{v_u}{\sqrt{2}} I(m_{b_1}^2, m_{b_2}^2, \mu^2).$$

where, $I(a, b, c) = -\frac{ab \ln(a/b) + bc \ln(b/c) + ca \ln(c/a)}{(a-b)(b-c)(c-a)}$.

- Δm_b (or Δy_b) is proportional to $\tan \beta$. **Large y_b for negative A'_b and large $\tan \beta$.**



MSSM (dashed line), NHSSM (Solid line);
 $\mu, M_1, M_2 = 200, 500, 1100$ GeV, $\mu' = 0$.



Sbottom-electroweakino couplings

The decay rates will essentially be proportional to $C_L^2 + C_R^2$ where C_L, C_R appear in the expression for couplings as given below.

For \tilde{b}_i - b - $\tilde{\chi}_1^0$ coupling:

$$C_L = -\frac{i}{6}(-3\sqrt{2}g_2 N_{12}^* Z_{i3}^d + 6N_{13}y_b Z_{i6}^d + \sqrt{2}g_1 N_{11} Z_{i3}^d),$$
$$C_R = -\frac{i}{3}(3y_b Z_{i3}^d N_{13} + \sqrt{2}g_1 Z_{i6}^d N_{11}).$$

For \tilde{b}_i - t - $\tilde{\chi}_1^-$ coupling:

$$C_L = i(y_t Z_{i3}^d V_{12}),$$
$$C_R = i(-g_2 U_{11}^* Z_{i3}^d + U_{12}^* y_b Z_{i6}^d).$$

N_{ij} are elements of neutralino diagonalizing matrix elements. N_{13}, N_{14} will be large for higgsino dominated LSP. Z_{ij} 's are for squark diagonalizing matrix elements where large Z_{i3} and Z_{i6} would mean large L and R-components in \tilde{b}_i for $i = 1, 2$.

- ▶ We consider higgsino like $\tilde{\chi}_1^0$ and $\tilde{\chi}_1^\pm$.
- ▶ For $\tilde{b}_i \rightarrow b\tilde{\chi}_1^0$ both C_L and C_R are approximately proportional to y_b .
- ▶ For $\tilde{b}_i \rightarrow t\tilde{\chi}_1^-$, couplings for L-type \tilde{b}_i is $\propto y_t$ whereas for R-like \tilde{b}_i coupling will be $\propto y_b$.
- ▶ A left like \tilde{b}_i will largely decay via $t\tilde{\chi}_1^-$. Thus it will have a smaller Branching fraction for $b\tilde{\chi}_{1,2}^0$.
- ▶ NHSSM for non-vanishing A_b' may be associated with a large y_b and this will cause a significantly different behaviour with respect to MSSM.
- ▶ We ignored $\tilde{b}_1 \rightarrow \tilde{t}_1 W^-$ kinematically by the choice of $m_{\tilde{b}_1} < m_{\tilde{t}_1} + m_W$.

Sbottom-electroweakino couplings

For \tilde{b}_i - b - $\tilde{\chi}_1^0$ coupling:

$$C_L = -\frac{i}{6}(-3\sqrt{2}g_2 N_{12}^* Z_{i3}^d + 6N_{13} y_b Z_{i6}^d + \sqrt{2}g_1 N_{11} Z_{i3}^d),$$

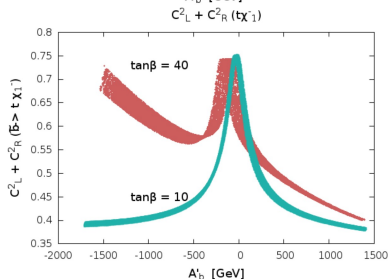
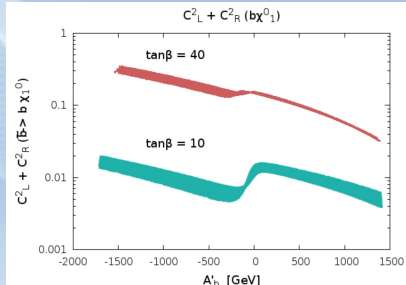
$$C_R = -\frac{i}{3}(3y_b Z_{i3}^d N_{13} + \sqrt{2}g_1 Z_{i6}^d N_{11}).$$

For \tilde{b}_i - t - $\tilde{\chi}_1^-$ coupling:

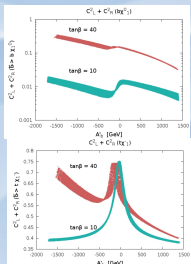
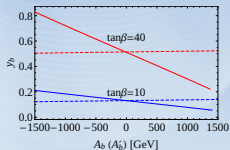
$$C_L = i(y_t Z_{i3}^d V_{12}),$$

$$C_R = i(-g_2 U_{11}^* Z_{i3}^d + U_{12}^* y_b Z_{i6}^d).$$

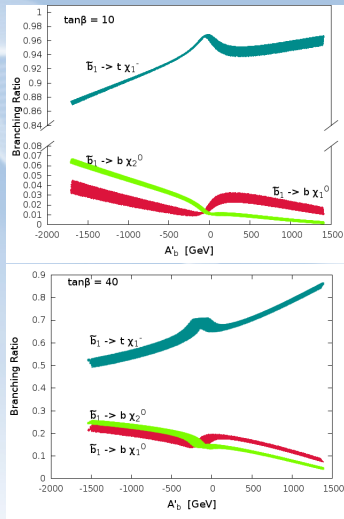
- ▶ Spread appears due to $100 < \mu < 350$ GeV. Region around $\mu + A'_b \simeq 0$ refers to scenarios of \tilde{b}_1, \tilde{b}_2 to be Left and Right like with negligible mixing. Large non-vanishing A'_b zones refer to larger mixing.
- ▶ For $\tilde{b}_i \rightarrow b\tilde{\chi}_1^0$, a change of sign of Z_{13}^d occurs near the no mixing zone. y_b enhancement/suppression occurs for negative/positive A'_b especially for large $\tan\beta$.
- ▶ For $\tilde{b}_i \rightarrow t\tilde{\chi}_1^-$, the central region for \tilde{b}_1 is Left like, hence peaked due to y_t irrespective of $\tan\beta$. For large negative A'_b and large $\tan\beta$ y_b enhancement effect is seen in the left zone. For the small $\tan\beta$ case, y_t dominates over y_b .



Branching ratios



- ▶ $\text{Br}(\tilde{b}_1 \rightarrow b\tilde{\chi}_1^0)$ essentially follows the profile of the couplings.
- ▶ When \tilde{b}_1 is left dominated (central region) the $\tilde{b}_1 \rightarrow t\tilde{\chi}_1^-$ decay rate is driven by y_t , hence becomes large.
- ▶ Difference of rates gets smaller for increase in y_b i.e. large negative A'_b and large $\tan\beta$ cases where competition sets in between the modes.

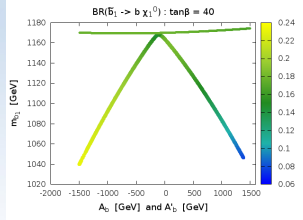
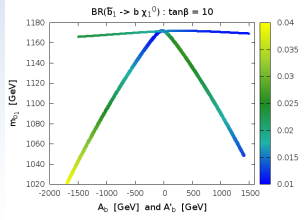
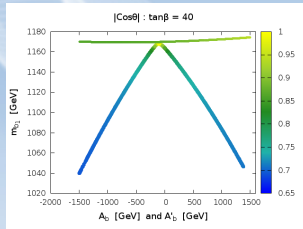
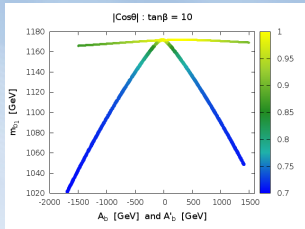


Masses, Mixing and Branching ratios in MSSM and NHSSM

$\mu, M_1, M_2 = 200, 500, 1100$ GeV

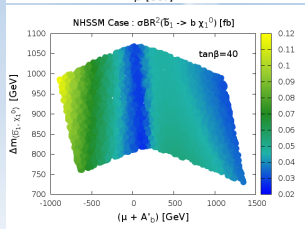
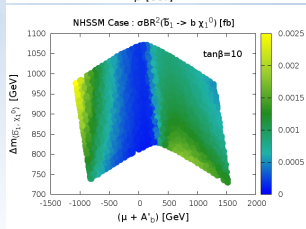
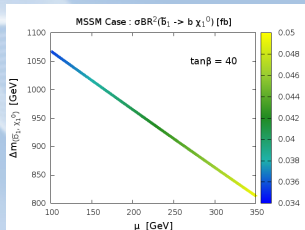
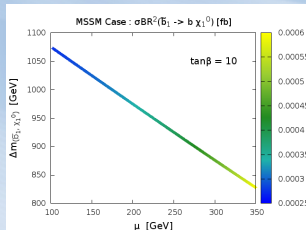
$m_{\tilde{Q}_3} = m_{\tilde{t}_L} = m_{\tilde{b}_L} = m_{\tilde{b}_R} (m_{\tilde{D}_3}) = 1.2$ TeV and $m_{\tilde{t}_R} (m_{\tilde{U}_3}) = 1.5$ TeV

Large mixing in NHSSM cases compared to MSSM (top flatter lines).



Signal Strength: Parton-level yields

$pp \rightarrow \tilde{b}_1 \tilde{b}_1^*$ at LHC 13 TeV, $\tilde{b}_1 \rightarrow b \tilde{\chi}_1^0$ leading to $2b + \cancel{E}_T$.



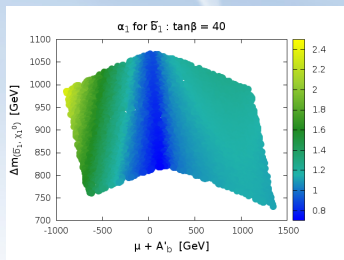
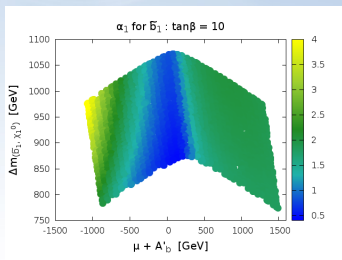
With $A_b = 0$, $(\mu + A'_b) \tan\beta$ controls the L-R mixing in NHSSM. Blue central regions refer to larger $\text{Br}(\tilde{b}_1 \rightarrow t \tilde{\chi}_1^-)$ since $\tilde{b}_1 \sim \tilde{b}_L \Rightarrow$ suppressed $\text{Br}(\tilde{b}_1 \rightarrow b \tilde{\chi}_1^0)$. NHSSM can give a much higher yield for a large $\tan\beta$.

Ratio of yields for \tilde{b}_1

$100 < \mu < 350$ GeV and $|A'_b| < 1.2$ TeV.

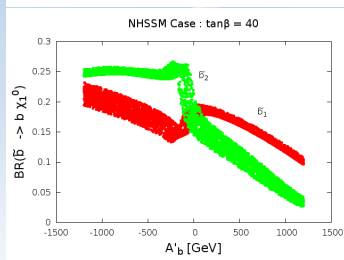
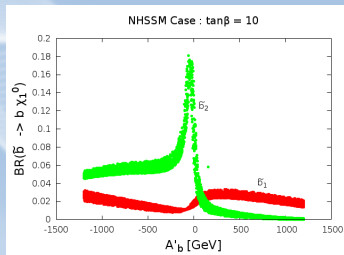
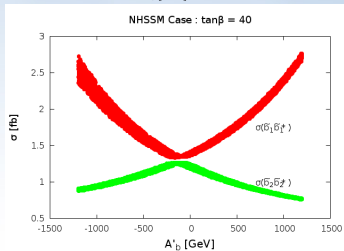
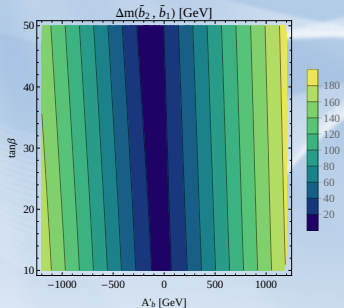
$$\alpha_1(A'_b) = \frac{[(\sigma_{\tilde{b}_1\tilde{b}_1} \times \text{BR}[\tilde{b}_1 \rightarrow b\tilde{\chi}_1^0])^2]^{\text{NHSSM}}}{[(\sigma_{\tilde{b}_1\tilde{b}_1} \times \text{BR}[\tilde{b}_1 \rightarrow b\tilde{\chi}_1^0])^2]^{\text{MSSM}}}$$

Ratio α_1 refers to same value of μ for MSSM and NHSSM. There is about an 8-fold increase from the lowest to the highest value for $\tan\beta = 10$ and around a 6-fold increase for $\tan\beta = 40$. Largest regions of α_1 fall in the negative large A'_b zone due to y_b -enhancement.



Including \tilde{b}_2 in the picture

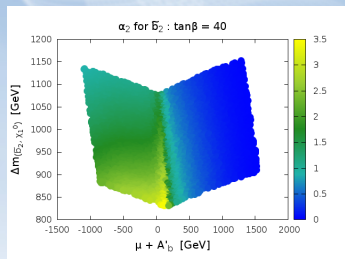
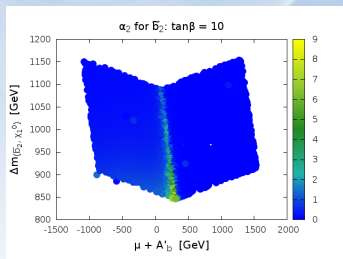
Because of the parameter choice, the mass difference of \tilde{b}_1 and \tilde{b}_2 is hardly very large.



$\tilde{b}_2 \simeq \tilde{b}_R$ near $A'_b = 0$ that suppresses $\text{Br}(\tilde{b}_2 \rightarrow t\tilde{\chi}_1^-)$ in favour of $\text{Br}(\tilde{b}_2 \rightarrow b\tilde{\chi}_1^0)$.

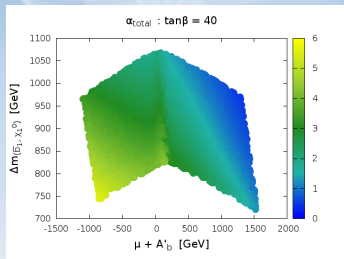
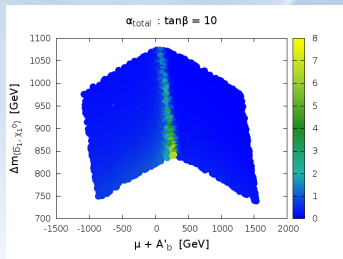
Ratio of yields for \tilde{b}_2

$$\alpha_2(A'_b) = \frac{[(\sigma_{\tilde{b}_2\tilde{b}_2} \times \text{BR}[\tilde{b}_2 \rightarrow b\tilde{\chi}_1^0])^2]^{\text{NHSSM}}}{[(\sigma_{\tilde{b}_2\tilde{b}_2} \times \text{BR}[\tilde{b}_2 \rightarrow b\tilde{\chi}_1^0])^2]^{\text{MSSM}}}$$



Ratio of yields for \tilde{b}_1 plus \tilde{b}_2

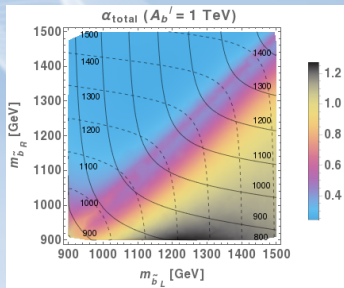
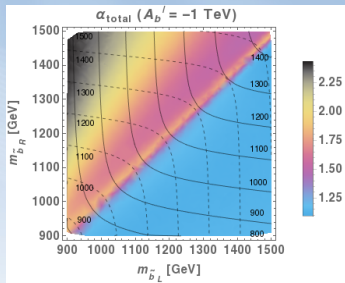
$$\alpha_{\text{total}}(A'_b) = \frac{\sum_{i=1,2} [(\sigma_{\tilde{b}_i \tilde{b}_i} \times \text{BR}[\tilde{b}_i \rightarrow b\tilde{\chi}_1^0])^{\text{NHSSM}}]}{\sum_{i=1,2} [(\sigma_{\tilde{b}_i \tilde{b}_i} \times \text{BR}[\tilde{b}_i \rightarrow b\tilde{\chi}_1^0])^{\text{MSSM}}]}$$



Up to eight-fold (six-fold) increased rates could be possible for $\tan\beta = 10$ (40) over the expected MSSM rates in the final state under consideration.

α_{total} for varying L and R sbottom masses

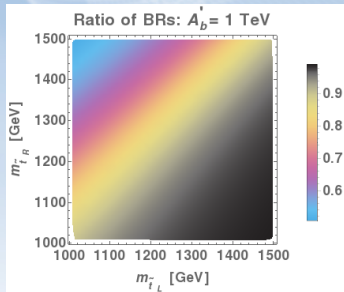
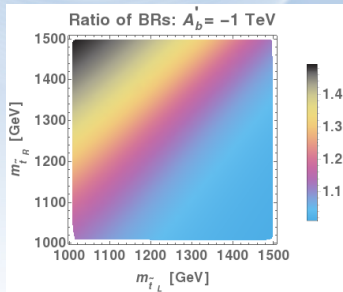
Variations of α_{total} in the $m_{\tilde{b}_L} - m_{\tilde{b}_R}$ plane for $A'_b = -1$ TeV (left) and $A'_b = 1$ TeV (right) and for fixed values of $\tan\beta$ ($=40$) and μ ($=200$ GeV). Contours of constant $m_{\tilde{b}_1}$ ($m_{\tilde{b}_2}$) are overlaid with solid (dashed) lines along the right (left) edges of the plots.



With A'_b large and negative the relative yield is more than unity in the left half of the diagonal. Largest α_{total} occurs near the black region in the upper left corner when the denominator for the MSSM value goes to a minimum. This happens via \tilde{b}_1 becoming further \tilde{b}_L -like than that of NHSSM (in which the mixing effect is larger due to A'_b).

Implications for stop searches

Generally, NHSSM involves a $\tan \beta$ suppression for stop mixing. However, $\tilde{t}_i - b - \tilde{\chi}_1^+$ vertex would indicate that a Left like stop would couple to a higgsino like chargino and a b-quark with strength y_b . Hence its decay rate would be different from that of MSSM depending on $\tan \beta$ and A'_b .
 $\tan \beta = 40$ and $\mu = 200$ GeV.



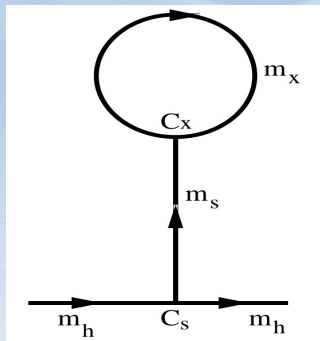
Conclusion

- ▶ Non-holomorphic MSSM is a simple extension of MSSM with a few virtues like it is able to isolate the electroweakino sector to some degree from the scalar sector. Hence, it is able to reduce the EW fine-tuning while allowing a higgsino type of $\tilde{\chi}_1^0$ to be a single component DM candidate.
- ▶ It can accommodate muon $g - 2$ result rather easily for some region of parameter space.
- ▶ It has unique signatures for the scalar sector especially for the down type of quarks and sleptons and it has some degree of influence on the Higgs sector too. It may have interesting signature on flavor physics.
- ▶ Distinguishing the signatures of NHSSM from MSSM can be challenging. However, the bottom Yukawa coupling may receive large radiative corrections and thus it may have some interesting consequences.
- ▶ A suitably designed multi-channel study may illuminate useful ways to distinguish the scenario from MSSM more effectively.
- ▶ Implications may be studied for suitable models by going beyond MSSM.

THANK YOU FOR YOUR ATTENTION

Backup pages

Tadpole correction



S : a singlet field. m_X : a very heavy scalar mass

Tadpole contribution: $\sim C_S C_X \frac{m_X^2}{m_S^2} \ln\left(\frac{m_X^2}{m_h^2}\right)$

If $m_S \ll m_X$ the tadpole contribution becomes very large.

For discussions: Ref. Hetherington, JHEP 2001

Hard SUSY breaking terms

S. Martin, Phys. Rev D., 2000; Possible non-holomorphic hard SUSY breaking terms:

Type	Term	Naive Suppression	Origin
hard	ϕ^4	$\frac{F}{M^2} \sim \frac{m_W}{M}$	$\frac{1}{M^2} [X\phi^4]_F$
	$\phi^3\phi^*$	$\frac{ F ^2}{M^4} \sim \frac{m_W^2}{M^2}$	$\frac{1}{M^4} [XX^*\phi^3\phi^*]_D$
	$\phi^2\phi^{*2}$	$\frac{ F ^2}{M^4} \sim \frac{m_W^2}{M^2}$	$\frac{1}{M^4} [XX^*\phi^2\phi^{*2}]_D$
	$\phi\psi\psi$	$\frac{ F ^2}{M^4} \sim \frac{m_W^2}{M^2}$	$\frac{1}{M^4} [XX^*\phi D^\alpha\phi D_\alpha\phi]_D$
	$\phi^*\psi\psi$	$\frac{ F ^2}{M^4} \sim \frac{m_W^2}{M^2}$	$\frac{1}{M^4} [XX^*\phi^* D^\alpha\phi D_\alpha\phi]_D$
	$\phi\psi\lambda$	$\frac{ F ^2}{M^4} \sim \frac{m_W^2}{M^2}$	$\frac{1}{M^4} [XX^*\phi D^\alpha\phi W_\alpha]_D$
	$\phi^*\psi\lambda$	$\frac{ F ^2}{M^4} \sim \frac{m_W^2}{M^2}$	$\frac{1}{M^4} [XX^*\phi^* D^\alpha\phi W_\alpha]_D$
	$\phi\lambda\lambda$	$\frac{F}{M^2} \sim \frac{m_W}{M}$	$\frac{1}{M^2} [X\phi W^\alpha W_\alpha]_F$
	$\phi^*\lambda\lambda$	$\frac{ F ^2}{M^4} \sim \frac{m_W^2}{M^2}$	$\frac{1}{M^4} [XX^*\phi^* W^\alpha W_\alpha]_D$

Electroweak Fine-tuning Components

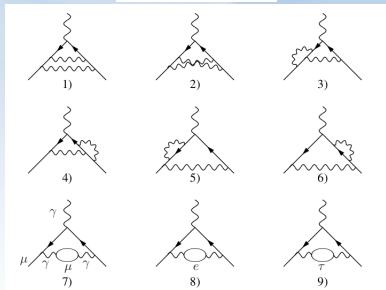
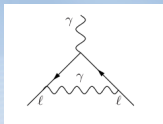
$$\begin{aligned}\Delta(\mu) &= \frac{4\mu^2}{m_Z^2} \left(1 + \frac{m_A^2 + m_Z^2}{m_A^2} \tan^2 2\beta \right), \\ \Delta(b) &= \left(1 + \frac{m_A^2}{m_Z^2} \right) \tan^2 2\beta, \\ \Delta(m_{H_u}^2) &= \left| \frac{1}{2} \cos 2\beta + \frac{m_A^2}{m_Z^2} \cos^2 \beta - \frac{\mu^2}{m_Z^2} \right| \times \left(1 - \frac{1}{\cos 2\beta} + \frac{m_A^2 + m_Z^2}{m_A^2} \tan^2 2\beta \right), \\ \Delta(m_{H_d}^2) &= \left| -\frac{1}{2} \cos 2\beta + \frac{m_A^2}{m_Z^2} \sin^2 \beta - \frac{\mu^2}{m_Z^2} \right| \times \left| 1 + \frac{1}{\cos 2\beta} + \frac{m_A^2 + m_Z^2}{m_A^2} \tan^2 2\beta \right|,\end{aligned}$$

$$\Delta_{Total} = \sqrt{\sum_i \Delta_{p_i}^2}, \quad (1)$$

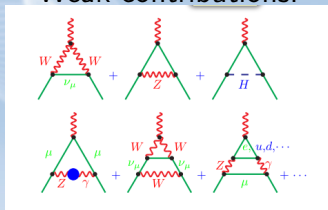
Ref. Perelstein, Spethmann: JHEP 2007, hep-ph/0702038

SM contributions: a_μ^{SM}

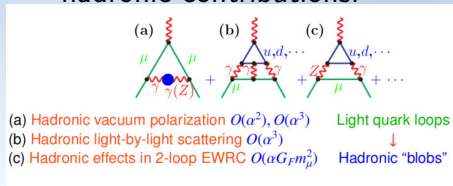
1 and 2-loop QED:



Weak contributions:



hadronic contributions:



Br($B \rightarrow X_s + \gamma$) in MSSM

- ▶ SM contribution (almost saturates the experimental value) $\rightarrow t - W^\pm$ loop.

- ▶ MSSM contribution:

1. $\tilde{\chi}^\pm - \tilde{t}$ loop:

$$BR(b \rightarrow s\gamma)|_{\tilde{\chi}^\pm} = \mu A_t \tan\beta f(m_{\tilde{t}_1}, m_{\tilde{t}_2}, m_{\tilde{\chi}^\pm}) \frac{m_b}{v(1+\Delta m_b)}$$

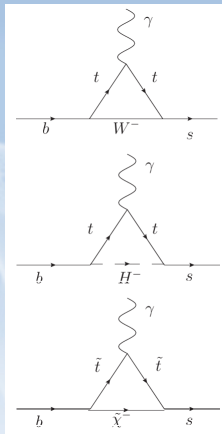
2. $H^\pm - t$ loop:

$$BR(b \rightarrow s\gamma)|_{H^\pm} = \frac{m_b(y_t \cos\beta - \delta y_t \sin\beta)}{v \cos\beta (1+\Delta m_b)} g(m_{H^\pm}, m_t)$$

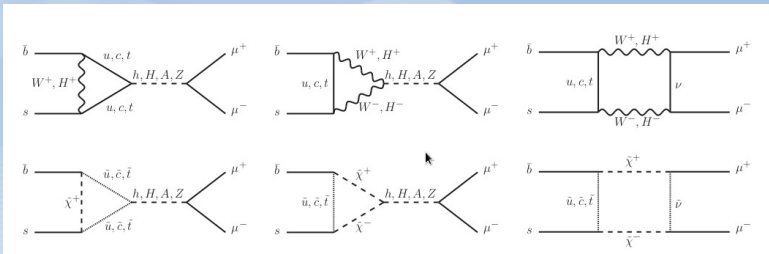
where,

$$\begin{aligned} \delta y_t &= y_t \frac{2\alpha_s}{3\pi} \mu M_{\tilde{g}} \tan\beta [\cos^2\theta_t I(m_{\tilde{s}_L}, m_{\tilde{t}_2}, M_{\tilde{g}}) \\ &+ \sin^2\theta_t I(m_{\tilde{s}_L}, m_{\tilde{t}_1}, M_{\tilde{g}})] \end{aligned}$$

- ▶ Destructive interference for $A_t \mu < 0 \rightarrow$ preferred.
- ▶ NLO contributions (from squark-gluino loops: due to the corrections of top and bottom Yukawa couplings) become important at large μ or large $\tan\beta$.



$B_s \rightarrow \mu^+ \mu^-$ in MSSM



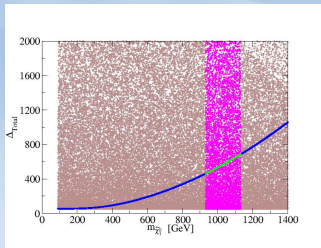
- ▶ Dominant SM contribution from : Z penguin top loop & W box diagram.
- ▶ SM value : $BR(B_s \rightarrow \mu^+ \mu^-) = 3.23 \pm 0.27 \times 10^{-9}$.
- ▶ LHCb result : $3.2_{-1.2}^{+1.4}(\text{stat.})_{-0.3}^{+0.5}(\text{syst.}) \rightarrow$ no room for large deviation.
- ▶ $BR(B_s \rightarrow \mu^+ \mu^-)_{SUSY} \propto \frac{\tan^6 \beta}{m_A^4}$

NH terms affecting or not affecting muon g-2 in two benchmark points where $\tilde{\chi}_1^0$ is bino-like

Table 1. Benchmark points for NHSSM. Masses are shown in GeV. Only the two NHSSM benchmark points shown satisfy the phenomenological constraint of Higgs mass, dark matter relic density along with direct detection cross section, muon anomaly, $\text{Br}(B \rightarrow X_s + \gamma)$ and $\text{Br}(B_s \rightarrow \mu^+ \mu^-)$. The associated MSSM points are only given for comparison and do not necessarily satisfy all the above constraints.

Parameters	MSSM	NHSSM	MSSM	NHSSM
$m_{1,2,3}$	472, 1500, 1450	472, 1500, 1450	243, 250, 1450	243, 250, 1450
$m_{\tilde{Q}_3}/m_{\tilde{U}_3}/m_{\tilde{D}_3}$	1000	1000	1000	1000
$m_{\tilde{Q}_2}/m_{\tilde{U}_2}/m_{\tilde{D}_2}$	1000	1000	1000	1000
$m_{\tilde{Q}_1}/m_{\tilde{U}_1}/m_{\tilde{D}_1}$	1000	1000	1000	1000
$m_{\tilde{L}_3}/m_{\tilde{E}_3}$	2236	2236	1000	1000
$m_{\tilde{L}_2}/m_{\tilde{E}_2}$	592	592	500	500
$m_{\tilde{L}_1}/m_{\tilde{E}_1}$	592	592	500	500
A_t, A_b, A_τ	-1500, 0, 0	-1500, 0, 0	-1368.1, 0, 0	-1368.1, 0, 0
A'_t, A'_μ, A'_τ	0, 0, 0	2234, 169, 0	0, 0, 0	3000, 200, 0
$\tan \beta$	10	10	40	40
μ	500	500	390.8	390.8
μ'	0	-175	0	1655.5
m_A	1000	1000	1000	1000
$m_{\tilde{g}}$	1438.9	1439.1	1438.9	1438.9
$m_{\tilde{t}_1}, m_{\tilde{t}_2}$	894.4, 1151.2	865.5, 1154.9	907.8, 1137.5	903.4, 1141.4
$m_{\tilde{b}_1}, m_{\tilde{b}_2}$	1032.4, 1046.2	1026.3, 1045.1	1013.8, 1051.2	1017.7, 1056.5
$m_{\tilde{\mu}_L}, m_{\tilde{\nu}_\tau}$	596.4, 596.3	573.5, 595.9	502.0, 497.1	465.8, 496.3
$m_{\tilde{\tau}_1}, m_{\tilde{\nu}_\tau}$	2237.1, 2238.5	2237.1, 2238.5	985.4, 997.2	988.5, 998.8
$m_{\tilde{\chi}_1^\pm}, m_{\tilde{\chi}_2^\pm}$	504.2, 1483.6	677.6, 1484.7	244.6, 421.0	262.3, 1255.2
$m_{\tilde{\chi}_1^0}, m_{\tilde{\chi}_2^0}$	448.6, 509.0	464.0, 680.6	231.3, 249.9	240.9, 262.1
$m_{\tilde{\chi}_3^0}, m_{\tilde{\chi}_4^0}$	522.6, 1483.5	683.2, 1484.7	400.7, 421.0	1253.3, 1253.7
m_{H^\pm}	1011.9	1005.8	955.7	1011.6
m_H, m_h	1008.1, 121.4	984.8, 122.8	948.0, 122.4	990.2, 122.8
$\text{Br}(B \rightarrow X_s + \gamma)$	3.00×10^{-4}	3.01×10^{-4}	2.01×10^{-4}	4.05×10^{-4}
$\text{Br}(B_s \rightarrow \mu^+ \mu^-)$	3.40×10^{-9}	3.45×10^{-9}	5.06×10^{-9}	1.65×10^{-9}
a_μ	1.94×10^{-10}	22.3×10^{-10}	34.8×10^{-10}	35.8×10^{-10}
$\Omega_{\tilde{\chi}_1^0} h^2$	0.035	0.095	0.0114	0.122
$\sigma_{\tilde{\chi}_1^0 p}^{\text{SI}}$ in pb	4.01×10^{-9}	3.47×10^{-10}	6.79×10^{-9}	3.15×10^{-12}

Electroweak fine-tuning and higgsino dark matter

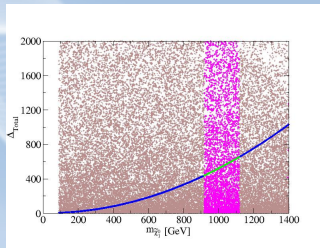


Δ_{Total} vs $m_{\tilde{\chi}_1^0}$ for $\tan\beta = 10$

MSSM (i.e. with $\mu' = A'_t = 0$): Thin blue line and partly green line in the middle. Δ_{Total} is little above 400.

NHSSM: brown and magenta. Consistent region satisfying a 3σ level of WMAP/PANCK constraints are shown. EWFT in NHSSM ranges from too high to too low (~ 50).

EW fine-tuning differs from FT estimate in UV complete scenario like CMSSM with NH terms. There, an FT expression would depend on NH parameters. The FT related low scale parameters p_i are no longer independent. NH+CMSSM still has FT estimate dominantly controlled by μ^2 (Ross *et. al.* 2016, 2017).



Δ_{Total} vs $m_{\tilde{\chi}_1^0}$ for $\tan\beta = 40$

EWFT in NHSSM can be vanishingly small.

- $-3 \text{ TeV} < \mu, \mu' < 3 \text{ TeV}$
- $-3 \text{ TeV} < A_t, A'_t < 3 \text{ TeV}$